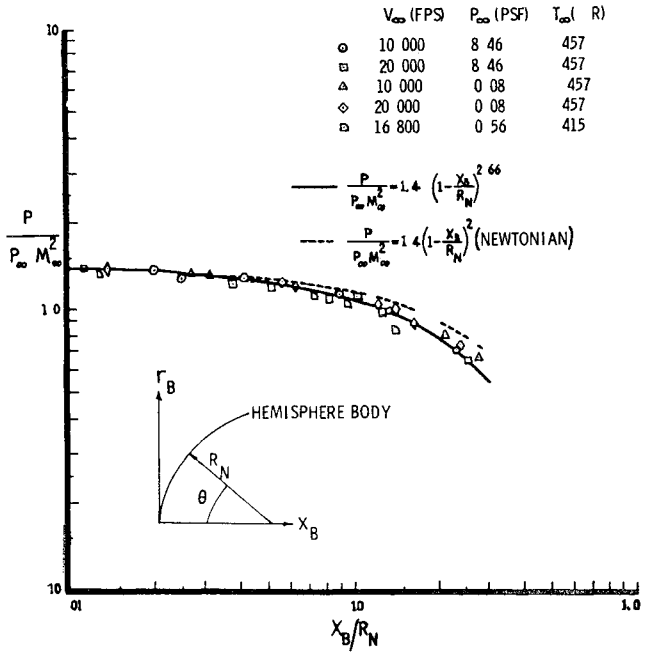

Fig 4 Hypersonic surface pressure distribution correlation in 0 5CO_2-0 25N_2-0 25A

For a particular Mars entry situation, typical of those currently being considered, the shock layer is presented in Figs 1 and 2 It is interesting to note that a radiation intensity peak occurs between the shock wave and the body Several cases, with various freestream velocities and densities, have been run In Fig 3, the shock-shape results from these calculations are correlated and compared with the Van Hise correlation [7] The surface pressure distributions are correlated in Fig 4 and compared with the Newtonian pressure distribution For the conditions considered here, quite good correlations are possible for the atmosphere 0 5 CO_2-0 25N_2-0 25A Some deviation is observed from the Van Hise air correlation in the case of shock shape and from the Newtonian pressure It remains to be seen what correlations are possible for other atmospheres The hypersonic approximation for shock standoff distance

$$\frac{\Delta}{R} = 1 - \frac{R_N}{R_s} = \frac{\epsilon}{1 + (\frac{8}{3}\epsilon)^{1/2}}$$

is plotted in Fig 5 (R = shock radius, R_N = body radius, Δ = standoff distance, and ϵ = density ratio across a normal shock) Results of the blunt-body calculations are also shown here As is expected, good agreement occurs for the higher velocities

More comprehensive calculations for a wide range of flight conditions and atmospheres are now being carried out and will be reported

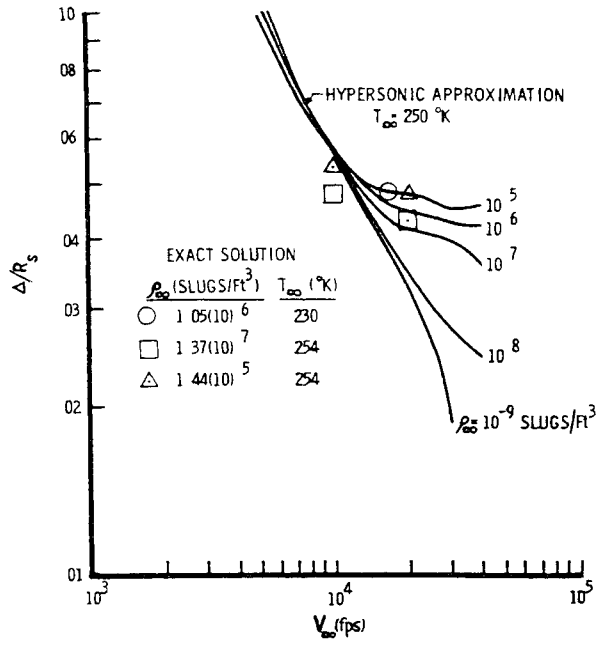

Fig 5 Hypersonic shock standoff distance in 0 5CO_2-0 25N_2-0 25A

References

[1] Eastman, D W, "Subsonic flow fields about blunt bodies by the inverse method," Boeing Co, Doc D2-35226 (October 21, 1963)

[2] Hayes, W D and Probstein, R F, *Hypersonic Flow Theory* (Academic Press, New York, 1959), p 230 ff

[3] Van Dyke M D and Gordon, H D, Supersonic flow past a family of blunt axisymmetric bodies," NASA TR R-1 (1959)

[4] Gardiner, C P, ' Equilibrium thermodynamic and radiative properties for gaseous CO_2 N_2-A mixtures of arbitrary composition," Boeing Co, Doc D2-22927 (to be released)

[5] White, W B, Johnson S M, and Dantzig, G B, "Chemical equilibrium in complex mixtures," J Chem Phys **28**, 751 (1958)

[6] Kivel, B and Bailey, K, ' Tables of radiation for high temperature air" Avco-Everett Research Lab RR21 (December 1957)

[7] Van Hise V, "Analytic study of induced pressures on long bodies of revolution with varying nose bluntness at hypersonic speeds," NASA TR R-78 (1960)

Temperature-Entropy Diagram of Monomethylhydrazine

FRANK BIZJAK* AND DONALD F STAI†
North American Aviation, Inc, Downey, Calif

Nomenclature

C_p = heat capacity at constant pressure, Btu/lbm-°R
d = differential operator
∂ = partial differential operator
Δ = delta change in property
H = enthalpy, Btu/lbm
ln = natural logarithm
MW = molecular weight, lbm/lb-mole
P = pressure, psia
P_r = reduced pressure P/P
Q = quality of vapor-liquid or vapor solid mixture, weight fraction vapor
R = gas constant, 1 9865/MW, Btu/lbm-°R
S = entropy, Btu/lbm-°R
T = temperature °R
T_r = reduced temperature T/T
V = specific volume, ft³/lbm
Z = compressibility factor

Subscripts

1 = reference condition
2 = final condition
c = critical
f = fusion
i = ideal gas
l = liquid

Received January 16, 1964

* Specialist-Research, Propulsion Department, Space and Information Systems Division Member AIAA

† Engineer-Research, Propulsion Department, Space and Information Systems Division

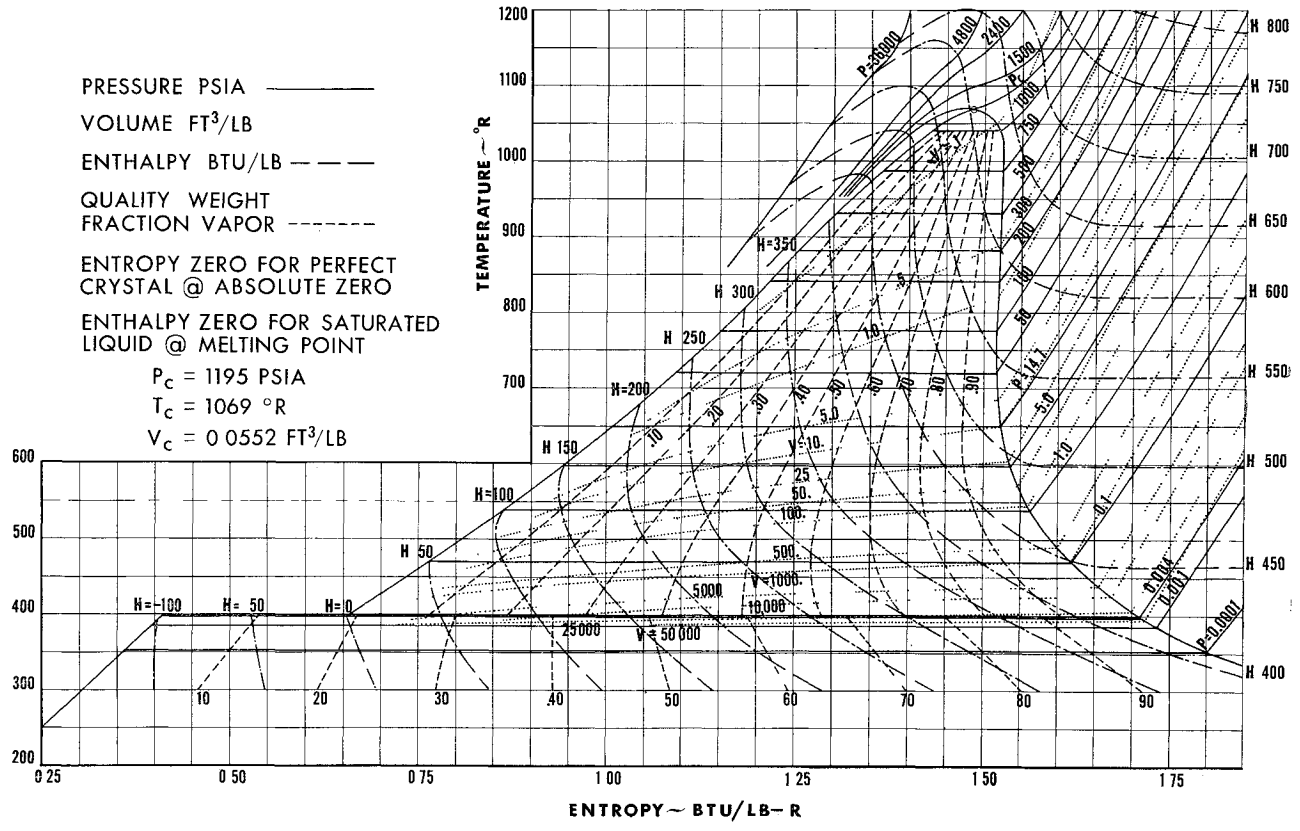

Fig 1 Temperature-entropy diagram for monomethylhydrazine

mix = vapor solid mixture
r = reduced
s = solid
sv = saturated vapor
T = temperature
v = vaporization

Introduction

AMONG storable propellants, monomethylhydrazine is of particular interest because of its wide liquid range and its relatively high specific impulse in combination with oxidizers such as nitrogen tetroxide Several problem areas in current space propulsion require knowledge of the hereto scattered and/or unavailable thermodynamic properties of monomethylhydrazine The expansion of propellants against low back pressure during the engine start may result in solid formation On engine shutdown, the expansion of residual propellant may result in unpredictable tail-off impulse After long engine operation, heat soakback from the engine may increase the propellant vapor pressure in the lines sufficiently to cause premature propellant vaporization To determine whether the effect of the monomethylhydrazine fuel in a given process is important or negligible and to evaluate this effect, the thermodynamic data for monomethylhydrazine were developed and are presented graphically in Fig 1 Large graphs of the diagram are available on request from the authors

Selection and Development of Data

Data on entropy for ideal monomethylhydrazine at 14 7 psia vs temperature have been reported in the literature [1] Applying nonideality corrections,[2] the real gas entropies at standard pressure were obtained The nonideality corrections at this pressure were within 0 28% of the ideal values

The saturated vapor entropies from the fusion to the critical temperature were derived from ideal entropies at standard pressure and vapor pressure data[3 4] and by the use of nonideality correction tables [2] The final values of the saturated vapor entropies were based on the equation

$$S = S_{iP_1} - R \ln(P_2/P_1) - (S_i - S)_{P_2\,T} \quad (1)$$

where the correction factor is given in terms of reduced properties

$$(S_i - S)_{P_2\,T} = -R \int_0^P \frac{(1 - Z)dP_r}{P_r} + RT \int_0^P \left(\frac{\partial Z}{\partial T_r}\right)_P \frac{dP_r}{P} \quad (2)$$

The saturated liquid line entropies were obtained from heat of evaporation data[4] and saturated vapor entropies as

$$S_l = S - \Delta S_v \quad (3)$$

where

$$\Delta S_v = \Delta H / T \quad (4)$$

The entropy of the solid was found from data of Aston, et al [3] and by graphical integration of the specific heat[3] represented by the equation

$$S_s = \int_0^T \frac{C_p dT}{T} = S_{T_1} + \int_{\ln T_1}^{\ln T_2} C_p \, d \ln T \quad (5)$$

Equations analogous to Eq (1) and (2) were used to derive entropy-pressure-temperature data for the superheated vapor region and in the region above the critical temperature and pressure Corresponding real gas entropy correction data were obtained from tables in Hougen, Watson, and Ragatz [2]

Enthalpy data of Lawrence[4] were expanded to obtain enthalpy at pressures above critical in the solid-vapor region and in the superheated vapor region For pressures above critical and for supersaturated and saturated vapor region,

$$H = H_i - [(H_i - H)/T\,]_T T_c \quad (6)$$

with

$$\left[\frac{(H_i - H)}{T}\right]_T = \left[RT^2 \int_0^P \left(\frac{\partial Z}{\partial T_r}\right)_P \frac{dP_r}{P_r}\right]_T \quad (7)$$

where the enthalpy of the fluid relative to that of its ideal gas at constant temperature $[(H_i - H)/T]_T$ is obtained from tables in Hougen, et al [2]

At the fusion point the enthalpy of the saturated liquid was defined as zero Along the triple-point line the enthalpy change is

$$\Delta H = T_f \Delta S \tag{8}$$

The enthalpy of solid-vapor mixtures below the fusion temperature was derived by iteration of the equation

$$H_{mix} = QH + (1 - Q)H \tag{9}$$

Specific volume data for the vapor phase were derived via the Wohl equation[5]:

$$P = \frac{RT}{V - B} - \frac{A}{T\ V(V - B)} + \frac{C}{V^3 T^{4/3}} \tag{10}$$

where $A = 6V^2P$, $B = 0\ 25\ V$, $C = 4V^3P$, and $R = 0\ 2329$ lb-ft^3/in^2-lbm-°R, with other symbols as defined under Nomenclature Equation (10) was solved by iteration with the help of a high-speed computer In the two-phase region, the specific volume of the saturated liquid was included in the computations

Results

The data developed is presented as a temperature-entropy diagram in Fig 1 The accuracy of the data is estimated to be within 0 5% near the ambient conditions The accuracy decreases when temperature and pressure approach and exceed the critical values, with a possible deviation of about 2%

References

[1] Liquid propellant manual," Liquid Propellant Information Agency, Applied Physics Lab , The Johns Hopkins Univ (December 1961) Unit 11, Figure 8

[2] Hougen O A , Watson, K M , and Ragatz, R A , *Chemical Process Principles, Part II, Thermodynamics* (John Wiley and Sons, Inc , New York 1959) 2nd ed , pp 584 585, 595–598 605–611

[3] Aston, J G , Fink, H L Janz, G J , and Russell, K E "The heat capacity heats of fusion and vaporization, vapor pressures entropy and thermodynamic functions of methylhydrazine, ' J Am Chem Soc **73,** 1939, 1941 (1951)

[4] Lawrence, R W , ' Handbook of the properties of UDMH and MMH,' Aerojet General Corp Rept 1292, Figure 4 and 10 (May 1958)

[5] Wilson E D and Ries, H C., *Principles of Chemical Engineering Thermodynamics* (McGraw-Hill Book Co , Inc , New York, 1956) p 238

Wake Transition

KWAN-SUN WEN*

General Electric Company, Philadelphia, Pa

IN this note, a correlation for hypersonic wake transition based on the freestream Mach number M_∞ and the freestream transition Reynold number $R_{\infty X_t}$ is made using the new wake data published by Avco/RAD,[1] some unpublished data by the Naval Ordnance Laboratory (NOL)[2 3] made available to this author, and data published previously by Massachusetts Institute of Technology (MIT)[4 5] and Graduate Aeronautical Laboratory, California Institute of Technology[6] The Avco/RAD data were obtained in a ballistic range with conical models of 10°, 15°, and 27½° half-angles The model velocities range between 4000 and 17,000 fps, and range pressures vary from 15 to 380 mm Hg in air The NOL data are for conical models of 6 3° and 8° half-angles, Mach numbers ranging from 8 to 14 7, and range pressures varying from 80 to 100 mm Hg in air

Slattery and Clay,[4 5] by plotting the transition distance vs a normalized pressure $P_N(P_N = p_\infty d/0\ 5)$, were able to reduce their transition data to curves roughly dependent only on P_N but independent of projectile velocity However, when the new data are plotted (Fig 1), they cannot be reduced in the same manner Therefore, certain dependence of the transition distance on the flight velocity is indicated by these new data

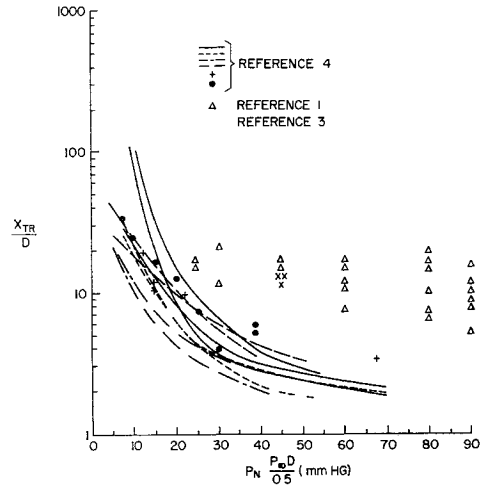

Fig 1 Variations of X_t/d with "normalized" pressure

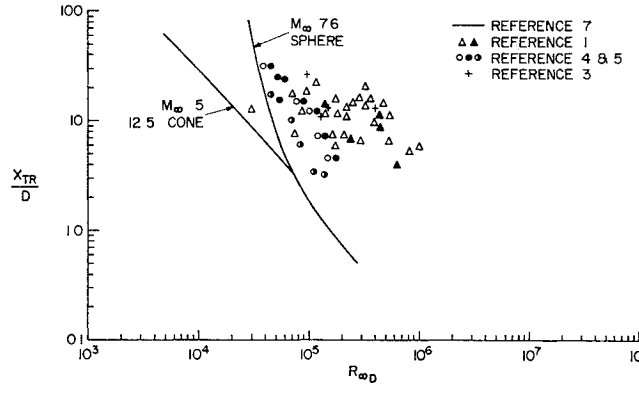

Fig 2 Variations of X_t/d vs $R_{\infty d}$

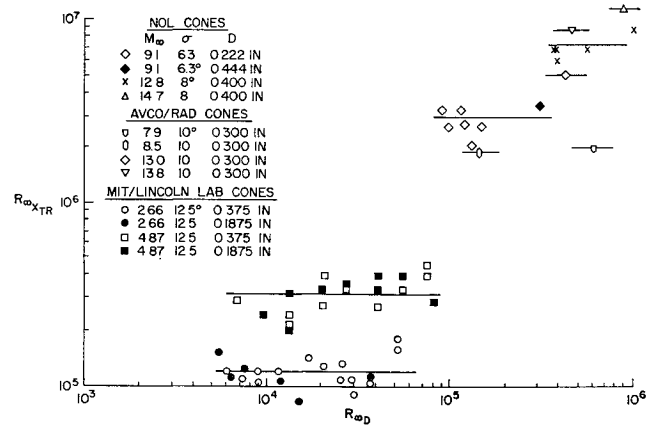

Fig 3 Variations of $R_{\infty X_t}$ vs $R_{\infty d}$ for cones (from Ref 2)

Received February 19, 1964 This work was done under Bell Telephone Laboratory Contract No DA-30-069 ORD-1955

* Research Engineer, Space Sciences Laboratory, Missile and Space Division Member AIAA